

# A Parallel Framework for Parametric Maximum Flow Problems in Image Segmentation

Vlad Olaru<sup>1</sup>

Mihai Florea<sup>1</sup>

Cristian Sminchisescu<sup>2,1</sup>

<sup>1</sup>*Institute of Mathematics of the Romanian Academy, <sup>2</sup>Lund University*

*vlad.olaru@imar.ro, mihai.florea@my.fmi.unibuc.ro, cristian.sminchisescu@math.lth.se*

## Abstract

*This paper presents a framework that supports the implementation of parallel solutions for the widespread parametric maximum flow computational routines used in image segmentation algorithms. The framework is based on supergraphs, a special construction combining several image graphs into a larger one, and works on various architectures (multi-core or GPU), either locally or remotely in a cluster of computing nodes. The framework can also be used for performance evaluation of parallel implementations of maximum flow algorithms. We present the case study of a state-of-the-art image segmentation algorithm based on graph cuts, Constrained Parametric Min-Cut (CPMC), that uses the parallel framework to solve parametric maximum flow problems, based on a GPU implementation of the well-known push-relabel algorithm. Our results indicate that real-time implementations based on the proposed techniques are possible.*

## 1 Introduction

Recent advances in image segmentation [10] (see figure 1) have led to improved accuracy over large and diverse image datasets [4, 18], by almost doubling the performance figures. This development has spurred the interest for the widespread use of image segmentation models as a component for key tasks in computer vision, such as video segmentation, large-scale applications for recognition and classification or mobile computing. In this context, of particular importance becomes the real-time performance of image segmentation algorithms. Although reliant on advanced methodology and data structures, the running time of the best performing algorithms still lags behind real-time, taking a few minutes for usual images, on average.

The most advanced image segmentation algorithms involve repeatedly solving multiple maximum-flow problems over monotonic schedules of parameter scales (parametric max-flow) constrained at image “seeds” corresponding to different locations in an image. Each image can be represented as a graph, where each pixel is a node connecting

locally with spatially adjacent ones (e.g. up, down, left and right), and connection strengths are modulated by pixel intensity similarity, or the presence of image contours. Solving each max-flow problem for one setting of the parameters is equivalent to computing a binary partition on the image graph. Performed systematically, at different locations and for monotonic schedules of parameters, it has been empirically observed that the process generates multiple binary segmentation hypotheses with good spatial overlap with the different objects and scene structures present in images (see figure 1). Often, the hypothesis generation is initiated from different seeds (see figure 3) independently, suggesting an inherently high degree of parallelism. Therefore, a trivially parallel implementation that generates solutions by running parametric maximum flow [13, 16] independently for each seed seems appropriate.



**Figure 1.** Original image, pool of segments generated by a max-flow segmentation algorithm, and ground truth respectively (best seen in color).

However, the intensive computational cost of generating segment hypotheses once a location (seed) has been selected suggests parallelizing the parametric maximum flow procedure as an alternative way to speed up image segmentation. Currently, there are no available parallel implementations of a parametric maximum flow algorithm, to the best of our knowledge. In this paper, we present the design of a general framework that can use existing parallel graph cut solutions such as GridCut [1] or CUDA NPPI [2, 3] to implement a parallel algorithm that approximates parametric maximum flow behavior. To this end, we use supergraphs, a special type of graphs that combine together several graphs, each of which has edge weights (or capacities) that depend on a different parameter.

The framework is general in terms of the architectures it can use. Supergraphs can run on multi-core architectures or GPU boards, either locally or cluster-wide. A parametric maximum flow problem encoded as a collection of supergraph cut problems can be scheduled dynamically to run on a heterogeneous collection of computing nodes. The dynamic scheduler adapts not only to the imbalances induced by the heterogeneous architectures used, but also to those intrinsic to the problem, as each problem takes a different, hardly predictable, amount of time.

The paper also presents a case study of a state-of-the-art image segmentation algorithm, Constrained Parametric Min-Cut (CPMC) [10], that uses the parallel framework with NVIDIA's GPU implementation of the well-known push-relabel maximum flow algorithm [14]. We then compare our solution to that of CPMC using a sequential pseudoflow algorithm [16] in a trivially parallel setup in which different instances of a segmentation problem are executed independently on several cores of a processor. In this way we seek how close can we get to a real-time solution for image segmentation.

To summarize, the paper proposes three main contributions: **(1) a parallel solution for parametric maximum flow problems based on supergraphs** that can be used by image segmentation algorithms; **(2) a general, parallel framework for parametric maximum-flow problems** that can *(a) handle various hardware architectures* (multi-core or GPU), both locally and remote in a cluster, *(b) dynamically schedule problems* to achieve improved segmentation times, and *(c) act as a performance evaluation tool* by allowing the use of various implementations of parallel maximum flow algorithms; and **(3) a case study for a state-of-the-art image segmentation algorithm (CPMC)**.

The rest of the paper is organized as follows: §2 describes shortly previous work on graph cuts and image segmentation for a clear understanding of the concepts. In §3, we present the framework solutions to parallelize the parametric maximum flow algorithms, using supergraphs. §4 presents the results of our case study evaluation of CPMC. We conclude in §5.

## 2 Graph-Cut based Image Segmentation

Graph cuts can be used to segment an image into a foreground object and the rest of the image, usually referred to as background, in order to obtain a figure-ground segmentation. This is a form of binary classification, with 1 assigned to foreground pixels and 0 to background.

The binary inference (labeling) process is performed by running a maximum flow/minimum cut algorithm on a graph whose vertices represent the pixels in the image. Two special vertices, the *source*  $s$  and the *sink*  $t$  are connected to every vertex of the graph by means of weighted edges (see figure 2); the weights are called edge capacities. For image

segmentation, the source and sink are associated with the two labels that will be used to distinguish the foreground object from the background. The weights of the edges that link  $s$  and  $t$  to the graph vertices (the pixels) quantify a penalty expressing how correct is to assign that pixel to either of the two classes of labels represented by the source and the sink.

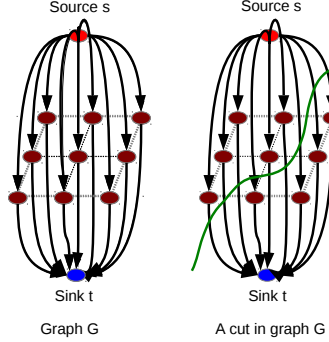


**Figure 2.** Associated image graph and cut example (best seen in colors).

Regular graph vertices (corresponding to image pixels) are linked to each other by weighted edges as well. Typically, image segmentation models use the weights of the edges that connect each vertex to its nearby neighbors (up, down and laterally) to model smoothness, i.e. the assumption that nearby pixels are likely to have similar labels.

An *s-t cut* of the graph is a partitioning of the vertices into two disjoint subsets: one containing vertex  $s$  and the other one containing vertex  $t$ . The *cost* of the cut is defined to be the sum of the weights of those edges in the graph that have one vertex in the  $s$ -partition and the other in the  $t$ -partition. A *minimum cut* corresponds to those graph cuts that have minimum cost.

A graph cut induces a labeling of the image pixels, depending on which partition they were inferred to. The problem of finding a cut is equivalent to the one of minimizing an energy defined on the graph. The energy has two terms, depending on which type of edges the cut crosses: edges linking either  $s$  or  $t$  to a regular vertex (pixel), or regular edges that link neighboring pixels. The first category of terms is called “data” or “unary” terms, while the second accounts for the “pairwise” terms (regularization terms). A minimum cut in such an image graph corresponds to a minimum energy among all of the possible label configurations of the image graph.

Greig et al. [15] have used this method for the first time to smooth noisy images and showed that the maximum a posteriori estimate of a binary image corresponds exactly to the maximum flow in the associated image graph constructed as previously described. According to the Ford and Fulkerson theorem [12], a maximum flow from  $s$  to  $t$  *saturates* the sum of the capacities of a set of edges in the graph that partitions the vertices into two disjoint sets that actually correspond to a minimum cut in the graph.

There are many polynomial time algorithms that solve the maximum flow problem (see [11]), including augmenting path (Ford-Fulkerson [12]) and push-relabel [14] algorithms, but their presentation is beyond the scope of this paper. A particularly interesting augmenting path algorithm widely used in computer vision is due to Boykov and Kolmogorov [7]. An extended view on the use of graph cuts in computer vision can be found in [8].

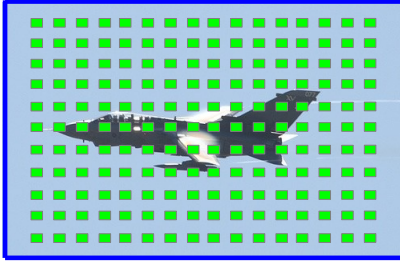


**Figure 3.** A regular grid of seeds in an image (best seen in color). Binary partitions (segmentations) are extracted around regularly placed foreground seeds (green dots) that express the foreground bias, while background seeds (in blue) are placed usually on the border of the image. Each generated segment corresponds to a graph cut segmentation problem. For an entire image, multiple independent solutions are generated at the cost of heavy graph cut computation.

## 2.1 Parametric Max Flow & Image Segmentation

Parametric max flow algorithms [13, 20] are used in image segmentation to generate a set of hypotheses for plausible object segments in a given image. Parametric maximum flow algorithms are able to optimize energies where the unknowns are both the binary labels of pixels and the weighting (scale)  $\lambda$  between the unary and pairwise terms of the energy model. The  $\lambda$  parameter values for which the corresponding energy value changes are called “breakpoints”. These breakpoints actually mark the optimal solutions of a parametric maximum flow problem. In the particular case, called “monotonic”, in which the factors that multiply the parameter  $\lambda$  in the unary (data) energy terms are all non-negative or non-positive, the optimal solutions are nested [13] and an efficient implementation of the parametric maximum flow algorithm is possible. The algorithms can either compute all breakpoints (an upper bound is the number of nodes in the graph) or a subset of them. In either case, the monotonicity makes the calculation significantly more efficient as earlier computations are reused. In practice, a preset list of parameter values (usually defined on a logarithmic scale), the so called  $\lambda$ -schedule, can be used instead of computing all the breakpoints, as empirical evaluations [10] have shown that the ground truth covering stays almost the same, at significantly lower computational costs due to the reduced number of breakpoints generated (and thus, a

reduced number of segment hypotheses). We say that this kind of run “approximates” parametric max flow behavior.

$\lambda$  values are associated with different seeds (preferably in a monotonic way) to generate a pool of segments with high probability of (foreground) object overlap. A seed is a set of pixels “frozen” to belong to either foreground or background. The foreground seeds are usually placed regularly on a grid in the image, whereas the background seeds are assigned on the borders of the image (see figure 3). A collection of maximum flow problems is solved for each pair of foreground and background seeds and different  $\lambda$  values (the  $\lambda$ -schedule), that are used to express the so called foreground bias associated with the non-seed pixels. The result is a large and diverse set of segments of different sizes and structural relevance.

## 2.2 Trivial Parallelism on Multi-Core Processors

A list of problems defined by a pair of foreground and background seeds and a  $\lambda$ -schedule can be easily solved independently on different processing units, given that no two pairs of foreground and background seeds are the same. For instance, a trivially parallel solution can be implemented by using MATLAB’s *parfor* instruction (or similar instructions in other languages) that executes each iteration independently as a thread on one of the available processor cores.

The main advantage of this type of parallelization is sim-

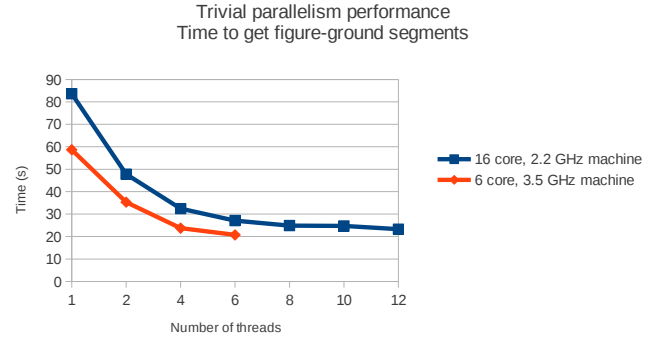


**Figure 4.** Trivial parallelism performance for figure-ground segmentations.

plicity, both in terms of programming effort and negligible need of synchronization of the worker threads (which should achieve maximum parallelism). From a programming point of view, there is little to be done beyond marking the appropriate *parfor* code blocks. The programming model is sequential for any particular *parfor* code block solving a problem, and the speed-up comes from the high usage of the available cores of the processor.

However, this parallel solution does not attempt to speed up any of the individual problems, which run as sequential algorithms. Figure 4 shows that, in practice, even with a relatively small number of processing units (cores), the speed-up of the trivially parallel solution gets quite soon bounded. The figure shows the time in seconds taken by CPMC to

yield figure-ground hypotheses for a given image, with a schedule of  $20 \lambda$  values and 178 seeds. This lack of scalability motivates the need to investigate parallel solutions for the parametric maximum flow solver as well, because, as it can be noticed, even on the faster processor the execution times are not close to real-time expectations.

### 3 Parallel Parametric Max Flow Solution

To the best of our knowledge, there is no available parallel implementation of a parametric maximum flow algorithm. In fact, there aren't many available parallel implementations of maximum flow algorithms. Some articles on the topic are available [17, 23], but don't offer the code. One available implementation is called GridCut [1], and works for multi-core processors only by defining a grid of computing units that can process graph cuts in parallel based on a popular augmenting path algorithm featuring tree-reuse [7]. GridCut implements adaptive bottom-up merging [21] and cache efficient memory layout [19]. Other available implementations of max flow algorithms are GPU implementations [2, 3, 24, 25]. The NVIDIA NPPI library [2, 3] implements a push-relabel algorithm [14].

Given the circumstances, running a parallel parametric maximum flow algorithm proves challenging. One solution would be to settle for an "approximation" of the parametric maximum flow behavior (in the sense defined in §2.1) by using a preset  $\lambda$ -schedule, and to run a parallel maximum flow routine once for each  $\lambda$  value in the schedule. However, this "batch" call is far from being optimal, since it is proven that, in a monotonic case, a parametric maximum flow algorithm can run asymptotically close to a regular maximum flow algorithm [13], i.e. they have the same theoretical complexity. Therefore, this batch procedure is only a poor match to what an optimal parallel parametric maximum flow algorithm could achieve in theory.

#### 3.1 Parametric Max Flow with Supergraphs

Besides the inability to optimize computations in the monotonic case, another shortcoming of the batch method is that running a single graph cut problem at the time, either on a multi-core processor or a GPU architecture, might not use the available hardware resources to the fullest. This aspect becomes striking especially for the latest generation of GPU boards (like those in NVIDIA's Tesla family) that feature thousands of computing cores.

To address the issue, consider running several graph cut problems simultaneously on the available parallel computing infrastructure. This is not a straightforward task, since the programming interfaces of parallel graph cut routines supplied by software like GridCut or CUDA NPPI take as a parameter a single graph. The solution is to "knit" together several graphs representing different problems into a larger graph, that we call a "supergraph", and to pass it on as a parameter of the graph cut calls.

These supergraphs represent the building block of our parallel framework for parametric max flow problems in image segmentation and can be constructed at two levels:  $\lambda$  and seed level. A  $\lambda$ -supergraph combines together graphs for several  $\lambda$  values, while a seed supergraph combines several  $\lambda$ -supergraphs together. Usually, the structures we work with combine an entire  $\lambda$ -schedule, the list of the  $\lambda$ s that we run the parametric max flow with, but it is possible to have smaller supergraphs as well. In the case of seed supergraphs though, we use only  $\lambda$ -supergraphs constructed for an entire  $\lambda$ -schedule.

Combining two graphs into a supergraph can be simply done by inserting additional vertices "between" the two graphs and by linking them to the regular vertices from the left and right graph by means of zero-weight edges (see figure 5). In terms of images, this procedure glues two images together, side by side, by inserting between them a set (a line) of pixels that do not relate in any way to their neighboring pixels in the joined images.

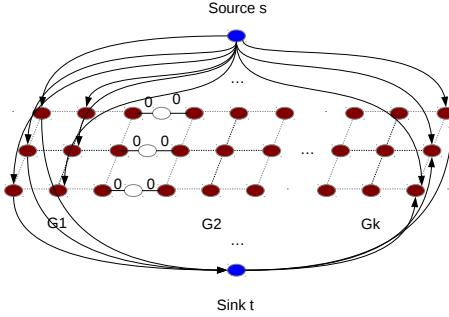


**Figure 5.** Supergraph composed out of  $k$  individual graphs  $G_1, G_2, \dots, G_k$  (best seen in colors).

Inductively, one can build arbitrarily large supergraphs out of individual graphs. Any minimum cut in a supergraph built like that is a union of the disjoint minimum cuts of the original graphs knitted together, plus some zero-weight edges that do not count towards the overall cost of the supergraph cut. Therefore, computing minimum energies associated with a pair of foreground-background seeds and a given  $\lambda$  value can be derived from such a supergraph by decomposing the minimum supergraph cut into its individual minimum cut components. Otherwise said, computing a supergraph maximum flow/minimum cut approximates the behavior of a parallel parametric maximum flow algorithm running on the individual graphs.

To see why this works, consider the following situation. Let  $S$  be a supergraph composed out of  $k$  individual graphs  $G_1, G_2, \dots, G_k$  (see figure 5). Let's assume  $C$  is a minimum cut in  $S$ , and  $C_1, C_2, \dots, C_k$  are the minimum cuts of the individual graph components. Suppose that one of the individual cuts, say  $C_i$ , is not a minimum cut in  $G_i$ . Then, there is a minimum cut  $C'_i$  in  $G_i$ , different than  $C_i$ . Since  $G_i$  is linked by means of zero weight edges to its neighboring graphs in  $S$ , any minimum supergraph cut that crosses

$G_i$  needs to include  $C'_i$ , because the zero-weight crossing edges do not contribute to the overall cost.  $C'_i$  is the minimum cost path severing  $G_i$  into two partitions and the supergraph cut must somehow cross  $G_i$ . Therefore, there is another supergraph cut including  $C'_i$  of smaller cost than  $C$ , which contradicts the assumption that  $C$  is a minimum supergraph cut. Thus, all of the  $C_i$ s must be minimum cuts in their corresponding  $G_i$ s.

Conversely, suppose that there is a supergraph cut  $C'$  in  $S$  whose cost is smaller than that of  $C$ . Then, there is another union of individual minimum cuts  $C'_1 \cup C'_2 \cup \dots \cup C'_k$  that compose  $C'$ . Since  $C'_i$ s are disjoint sets, it means that at least one of them from  $C'$ , say  $C'_j$ , is smaller than its corresponding  $C_j$ , which contradicts the assumption that  $C_j$  is a minimum cut in  $G_i$ .

Therefore, it is sound to use this procedure to amass several graphs into a supergraph and use the individual components of the minimum supergraph cut as individual minimum cuts. Thus, one can solve simultaneously either a single seed problem (by building a  $\lambda$ -supergraph) or several seed problems (by binding together several  $\lambda$ -supergraphs for several seeds). The ability to run custom sized graphs ends up in a better usage of the available computing power of the underlying hardware architecture.

We have used supergraphs both with GridCut and CUDA NPPI, but our CPMC case study focuses on the GPU solution, as our evaluations showed that GridCut performs much worse than CUDA. Nevertheless, we would like to point out that the supergraph method is general and can be used with any available parallel graph cut implementation as a means to compute a parametric maximum flow in parallel. The method is especially effective when the parallel graph cut source code is not available (e.g. CUDA NPPI).

## 3.2 Exposing More Supergraph Parallelism

It is known that exchanging the roles of source and sink, operation that we call an *s-t swap*, does not affect the results of a graph cut algorithm (i.e., the maximum flow/minimum cut remain the same). However, it might help a parallel implementation of a push-relabel algorithm, like NVIDIA's *nppiGraphcut* [2, 3], run faster [22]. The reason for this behavior is that the parallel workload at every iteration of the algorithm is given by the number of regular vertices (pixel nodes) that have residual capacity on their edges to/from source independent of the edges to/from sink [22]. So, if there are more such vertices for the sink than for the source, swapping them exposes more parallelism.

Choosing the source and the sink by running the algorithm twice, once with the original graph and then after an *s-t swap*, to see which run yields faster results, is obviously not a solution. Instead, we use an heuristic for choosing the source and the sink. For each regular vertex in the graph, the difference between the capacities of its source and sink

edges is computed. Then, for each vertex, we add separately the positive and negative differences. If the number of negative differences turns out to be larger than that of positive differences, we apply the *s-t swap*. This procedure helps have more hardware resources active per algorithm iteration and improves performance significantly (see §4.3).

When using *s-t swaps* with supergraphs, one has to pay attention to properly choose the source and sink so that every individual graph is aligned for maximum available parallelism. In other words, all the individual graphs composing a supergraph must be checked if they need to be *s-t swapped* so that the resulting supergraph has a source and a sink that allow the highest possible degree of parallelism. That is easier done for  $\lambda$ -supergraphs, because such a supergraph represents the same problem (i.e., the same foreground-background pair of seeds), but care must be taken when building seed supergraphs, that might need to reverse some of the individual  $\lambda$ -supergraphs.

## 3.3 Using the Parallel Framework

A collection of seed problems, each represented by a pair of foreground and background seeds and a  $\lambda$ -schedule, is going to be encoded by means of supergraphs, as previously described. The resulting set of supergraphs can have a smaller size than the collection of seed problems if several such problems are expressed by means of seed supergraphs. Each resulted supergraph gets scheduled for parametric maximum flow processing on a given computing node (also called server), either locally or remote. Remote processing is achieved by means of Remote Procedure Calls (RPC) for the supergraph cut routines. The scheduling is controlled by a master node, which is the node that runs the image segmentation algorithm. The master node can act as computing server as well, but in this case the local computing architecture, either CPU- or GPU-based, is going to be accessed directly instead of performing an RPC. The resulting cluster of servers that collaborate to solve the collection of seed problems may be heterogeneous, regardless whether we are talking about CPUs or GPUs.

### 3.3.1 Supergraph Scheduling

The master node can perform two types of scheduling: static and dynamic. Static scheduling assigns supergraphs to computing servers by using a MATLAB *parfor* instruction with  $n$  threads in which each parallel loop iteration  $i$  gets allocated task  $i \bmod n$ . All the tasks allocated to a class  $i \bmod n$ , for instance, those that execute an RPC to a given remote server, will be executed sequentially, one after the other. Thus, the makespan, the overall length of the task schedule, will be determined by the time needed to run the longest class  $i$  of tasks  $i \bmod n$ .

However, in a heterogeneous computing environment with different hardware architectures (for instance, different types of GPU boards, as in our case study), significant

computational load imbalances may arise. Even the same hardware, say two GPU boards of the same kind, will not yield the same performance when accessed locally vs. over the network via RPC. Moreover, there is an intrinsic source of imbalance in the segmentation problem, because different seeds of an image induce different image graphs and therefore different graph cut computational costs.

The dynamic scheduler is also multi-threaded and attempts to offset these load imbalances by picking up a server from a list of available servers in FIFO order and executing the RPC (or a local call, in the case of the master node) to that node with a supergraph as a parameter. The server is removed from the list and, later on, when the supergraph cut call finishes, is inserted back into the list. Hence, the list of available servers grows and shrinks dynamically and, at times, may become empty, in which case no server is available for computation and the master program dispatching the tasks gets blocked.

In contrast to static scheduling, this FIFO scheduling with a dynamically managed list of available servers, in which a given supergraph can be handled as soon as a server is available, offers a more balanced mix of task overlaps, which in turn should contribute to a shorter makespan. In theory, one might attempt to schedule supergraph cut computations ahead of time in order to optimize the schedule, if a priori knowledge about the supergraph cut computational loads would be available. This kind of information is hard to get though, because it is highly data dependent.

Technically, the scheduler code is written in MEX C and is multi-threaded. When a request for computing a supergraph maximum flow is issued, the MEX routine called by the MATLAB code computes the appropriate parameters of the call and hands over the job to a service thread supplied by a thread pool mechanism, so that the computation can proceed independently of other similar calls. Thread-safety is therefore mandatory on the client RPC (master) side, but not necessarily on the server side. However, particular aspects related to network communication turned out to make a case for multi-threaded RPC servers as well, as it can be seen in the next section.

The scalability of the framework depends on two main components: the scalability of the master scheduler and that of the parallel graph cut routine processing the supergraphs. For the latter, our framework is limited by the scalability of the available software used (i.e., GridCut, CUDA NPPI, etc). The scalability of the scheduler is influenced by the available resources on the master node and the network latency for remote communication. However, as our experiments show (see §4.7), achieving performance close to real-time doesn't necessarily assume many computing nodes. Therefore, one can conclude that the master scheduler shouldn't face scalability problems as long as it can use small-scale multiprocessor (8-16 cores) machines.

### 3.3.2 Supergraphs and Network Communication

Typical images sizes from the VOC dataset [4] that we use in our case study evaluation amount to roughly 80-100K pixels, and so are the sizes of the corresponding image graphs. Usually, for computational reasons, image segmentation algorithms like CPMC downsample images to half, so the resulting graph size sums up to approximately 160-400KB of memory (for 4-byte floats or integers). Packing several graphs of such sizes into a supergraph can enlarge the size of the RPC parameters even further. Moreover, library calls like NVIDIA's *nppiGraphcut* [2, 3] require five such large matrices as parameters among others. As a result, the overall size of the RPC parameters that have to be transferred over the network tends to be quite large and thus may have a negative impact on the performance of the call.

One possible solution to alleviate the consequences of transferring large amounts of data over the network is to minimize the number of transfers by packing several graphs into a larger supergraph (say, instead of sending a single  $\lambda$ -supergraph parameter, one might send a two seed supergraph, i.e. two  $\lambda$ -supergraphs). Thus, the overhead of the send/receive network operations gets amortized over larger amounts of data and the transfer performance increases. In conjunction with other mechanisms like the use of Jumbo Frames for Gigabit networks, supergraphs can thus help optimize communication as well. However, the overall occupied bandwidth is the same and a second call to the same server would have to wait until the entire previous RPC has finished, before it can start sending its own parameters.

A better usage of the available bandwidth would seek to overlap communication with computation. Once an RPC has been issued to a server, one can immediately issue a second one, counting on the fact that, while the first call gets executed on the remote server, the transfer of the parameters of the second call can proceed independently of the first call. Naturally, such a scenario requires multi-threaded server capabilities, in order to be able to handle two concurrent RPCs. In particular cases, such as the one in which a remote server hosts a single GPU board, there seems to be hardly the need to "piggyback" more than one RPC to the first call, since mutual exclusive access to the GPU board is required anyway. Thus, the advantage of using just two threads might be questionable. However, the reasoning may be extended to four threads, say, for a remote server hosting two GPU boards, and so on. So we implemented a multi-threaded RPC server as well, which has not been our first option, given the fact that the TIRPC package available in the current Linux distributions does not include multi-threaded support for server side RPC (unlike the original Sun Microsystems/Oracle version). But this choice turned out to be beneficial in our case study for CPMC using NVIDIA's NPPI library, even if we used a server with a single GPU board and only two server threads, as shown in the experimental evaluation.

## 4 Case Study: CPMC

The CPMC release [9] can use two parametric maximum flow algorithms [13, 16]. In our evaluation, we have chosen the pseudoflow algorithm [16] because it can also run “approximately” (see §2.1), i.e. without computing all the breakpoints, by accepting as argument a preset  $\lambda$ -schedule. Thus, the whole CPMC algorithm runs faster and the comparison to our framework is fair. The other option [6, 13] works only by computing all the breakpoints online.

In this setup, CPMC solves iteratively a list of independent problems defined by a pair of foreground and background seeds and a  $\lambda$ -schedule passed to the pseudoflow algorithm. The problem solver is implemented in MATLAB, while the pseudoflow solver implementation is done in C (and hooked up with the MATLAB code by means of MEX libraries). Thus, a trivially parallel solution can be implemented easily by using MATLAB’s *parfor* instruction that executes each iteration independently as a thread on one of the available processor cores (see figure 4).

Motivated by the argument in §2.2, we compared the pseudoflow based solution to that of the supergraph framework, in order to parallelize the figure-ground stage of CPMC [10] and to assess its utility as a tool towards real-time performance for image segmentation. To that end, we have employed a cluster of GPUs managed by the framework as described in §3.1 and §3.3. The GPU cards have run the push-relabel implementation of the NVIDIA NPPI library [2, 3]. With no access to the library source code, we had to use the NVIDIA code as a black box, with no possibility to perform any kind of code optimizations.

### 4.1 Evaluation Setup

The evaluation that follows has been driven on two types of HP workstations: three Z840 stations equipped with one Intel(R) Xeon(R) CPU E5-2620 v3 @ 2.40GHz processor (6 cores) and 32GB RAM, and one Z420 station equipped with an Intel(R) Xeon(R) CPU E5-1650 v2 @ 3.50GHz processor (6 cores) and 32 GB RAM. We had five NVIDIA GPUs at our disposal for the experiments, two Tesla K40 (one per Z840 station) and three Titan Black boards (two hosted on a Z840 machine, and the third on the Z420 station). A Tesla K40 board features 2880 cores clocked at 745MHz and 12 GB of RAM, while a Titan Black board has 2880 cores running at 889 MHz and 6 GB of RAM. We used CUDA 6.5 for the experiments. All the systems run Linux and are connected by Gigabit Ethernet.

Unless otherwise stated, all the experiments use a 400 images subset of the VOC2012 dataset [4] and evaluate over this subset of images the minimum, maximum and average time values taken by the graph cuts of the CPMC [10] figure-ground segmentation stage that yields the segment hypotheses. This stage uses three different Segmenter methods for a total of 178 seeds and 20  $\lambda$  values for each of these seeds (these are the default values, for details see [9]).

### 4.2 Performance of the Pseudoflow Algorithm

The first experiment attempts to assess the performance of the pseudoflow algorithm [16] on multi-core architectures. As already mentioned, this is a sequential parametric maximum flow algorithm and can be easily used with the *parfor* MATLAB instruction to implement a form of trivial parallelism on multi-core architectures. This parallel algorithm will represent our baseline performance.

	Time	Min	Avg	Max
1 parfor thread	13.35 s	46.33 s	72.59 s	
2 parfor threads	8.14 s	28.15 s	42.70 s	
4 parfor threads	5.35 s	17.63 s	26.23 s	
6 parfor threads	4.10 s	14.35 s	21.48 s	

**Table 1.** Parametric pseudoflow performance on multi-core architectures.

We ran CPMC with the pseudoflow solver on a 6-core Z840 workstation with a  $\lambda$ -schedule of 20 values by varying the number of threads of the *parfor* instruction from 1 to 6. The results are shown in table 1 and represent the average, maximum and minimum times for performing the graph cuts of the CPMC figure-ground segmentation stage. Please note that the average times follow the behavior seen in figure 4: after a significant drop when moving from one to two threads, the times do not continue to decrease at a similar rate and the effect of further increasing the number of threads doesn’t seem to pay off in the long run.

### 4.3 Basic Performance of Push Relabel on GPUs

Our next experiment on the VOC image subset attempts to shed some light on the basic, local (that is, no RPC) performance of our GPU cards. We ran the experiments on the Z840 workstations using  $\lambda$ -supergraphs (i.e., one seed supergraphs) with 20 values when calling the NVIDIA NPPI *nppiGraphcut* routine. The first two rows of table 2 present the results for the K40 and Titan Black boards. The third row of the table presents the results of using simultaneously both of the Titan Black cards in one of our Z840 stations. On average, the Titan Black board is roughly 14% faster than a K40 and almost 9% faster than the trivially parallel algorithm running single threaded (see table 1). It is also worth noting that two Titan Blacks together outperform the trivially parallel algorithm on two threads by roughly 21%. All these figures assume the use of supergraphs that are properly *s-t swapped* for optimal performance.

Rows 4 & 5 of table 2 show the performance figures of the two boards when using supergraphs without applying the *s-t swap* optimization (see §3.2). The comparison to the first two rows in table 2 shows that the *s-t swap* operation on supergraphs decreases the figure-ground segmentation latency by roughly 39% for Tesla K40 and 36% for Titan Black, on average. Also noteworthy is the maximum

latency value of supergraphs that don’t use *s-t swaps* when running on Titan Black boards, which shows how poor can be, at times, the degree of available parallelism if the source and sink are not swapped.

Time	Min	Avg	Max
Tesla K40	12.91 s	49.17 s	86 s
Titan Black	11.33 s	42.39 s	73.93 s
2 x Titan Black	5.19 s	22.37 s	45.90 s
K40 no ST swap	20.68 s	80.19 s	200.33 s
Titan B. no ST swap	16.67 s	66.10 s	932.82 s
Titan Black batch	47.25 s	116.47 s	211.76 s

**Table 2.** Performance of NVIDIA’s implementation of the push relabel algorithm on GPU boards.

The last row of table 2 shows the performance of the Titan Black board without using supergraphs at all (i.e., by using the “batch” procedure mentioned in §3 that calls iteratively the *nppiGraphCut* routine for every  $\lambda$  value in the schedule). A comparison between the average figures in the last two rows of the table shows that using supergraphs reduces the figure-ground segmentation latency almost to half compared to the batch method, thus making a strong case for the use of supergraphs. Please also note the minimal latencies, where supergraphs are almost three times faster than the batch method.

Time	Min	Avg	Max
1 seed	12.91 s	49.17 s	86 s
2 seeds	11.07 s	46.35 s	83.80 s
4 seeds	9.64 s	46.12 s	87.36 s

**Table 3.** Impact of seed supergraphs.

#### 4.4 Impact of Seed Supergraphs

Using seed supergraphs (see §3.1) should achieve better usage of the underlying hardware. In this section, we assess the performance of NVIDIA’s push relabel implementation on seed supergraphs when varying the number of seeds. Table 3 shows Tesla K40 results on a Z840 station for 1, 2 and 4 seeds respectively. All the supergraphs use a 20 value  $\lambda$ -schedule. Please note that larger supergraphs yield better results for our VOC image subset.

#### 4.5 RPC Performance

We also conducted experiments to evaluate the performance of our RPC version of the NVIDIA *nppiGraphcut* call to access remote GPU boards. The experiments have used Tesla K40 boards, Z840 workstations and  $\lambda$ -schedules of 20 values. The first row of table 4 presents the graph cut times to get the figure-ground segment hypotheses when using  $\lambda$ -supergraphs only. We also evaluated the optimizations discussed in §3.3.2. The second row shows the improvements obtained when using larger supergraphs (two

seeds vs. one as in the first table row) to make a better usage of the available network. The last row of the table shows the RPC performance with multi-threaded servers when two consecutive GPU RPCs are submitted to the same server in order to benefit from the overlap of communication with computation.

Time	Min	Avg	Max
1 seed	19.43 s	65.24 s	107.63 s
2 seeds	15.50 s	58.55 s	101.96 s
MT server	15.51 s	42.93 s	69.76 s

**Table 4.** Performance of remote GPU RPCs.

#### 4.6 Impact of the Host Architecture

The reported running times for figure-ground segmentation account for some host code as well, i.e. code that doesn’t run on GPU and prepares the matrices supplied as arguments to the *nppiGraphcut* call. This section exposes the impact of this code on the total time figures when using the fastest of our GPU boards, Titan Black according to table 2, on a Z840 station (equipped with a 6-core, 2.4 GHZ CPU) and on a Z420 station, respectively (equipped with a 6-core, 3.5 GHz CPU). Table 5 presents the running times for a  $\lambda$ -supergraph with 20 values. One can notice that the workstation with the faster processor, Z420, yields slightly better running times overall for our VOC image subset. Nonetheless, the difference is small enough to consider that, practically, the host code doesn’t affect significantly the overall time.

Time	Min	Avg	Max
Z840	11.33 s	42.39 s	73.93 s
Z420	11.40 s	41.61 s	71.69 s

**Table 5.** Impact of the host architecture on the performance of GPU-based graph cuts.

#### 4.7 Parametric Max Flow using Supergraphs and Clusters of GPUs

Once we assessed the performance of the individual hardware available and mechanisms we have presented in the paper, we proceeded to set up a cluster of GPUs that would act as a parallel, cluster-wide parametric maximum flow solver based on supergraphs. To this end, we used the information from the previous experiments and decided to use the Z840 workstation equipped with two Titan Black cards as a master node, since these cards are faster than the K40s and local access to them should be faster than by means of RPC. The other three stations, two Z840 equipped with one Tesla K40 card each and the Z420 machine hosting the third Titan Black board have been used to build the cluster of GPUs. We tested with  $\lambda$ -schedules with 20 and 10 values, both for a  $\lambda$  supergraph and a two-seed supergraph and compared the results with those of CPMC using

the pseudoflow solver on a 6-core Z840 machine. The comparisons are shown in tables 6 and 7 and reveal better overall times for the graph cuts of the figure-ground segmentation stage based on clusters of GPUs. In terms of average times, a GPU cluster using 20  $\lambda$ -supergraphs outperforms the trivially parallel solution using the pseudoflow algorithm by roughly 9%, whereas the use of two-seed supergraphs sets the performance gain around 15%. When halving the  $\lambda$ -schedule, the performance gains of the GPU based solutions amount to roughly 17% and 20%, respectively (see table 7).

Time	Min	Avg	Max
Pseudoflow 6 threads	4.10 s	14.35 s	21.48 s
GPU cluster 1 seed	3.99 s	13.06 s	21.98 s
GPU cluster 2 seeds	3.46 s	12.15 s	22.36 s

**Table 6.** The performance of GPU clusters (20  $\lambda$ -schedule) vs. the multi-core based solution.

Time	Min	Avg	Max
Pseudoflow 6 threads	3.79 s	11.36 s	16.21 s
GPU cluster 1 seed	2.93 s	9.42 s	15.52 s
GPU cluster 2 seeds	2.61 s	9.12 s	16.18 s

**Table 7.** The performance of GPU clusters (10  $\lambda$ -schedule) vs. the multi-core based solution.

#### 4.8 Graph Cut Accuracy

So far, our evaluations concerned running times, but CPMC and image segmentation algorithms in general need to fulfill their primary goal of accuracy in the first place. The accuracy of an image segmentation algorithm is influenced by several factors, the graph cut calculation accuracy being an important one. Therefore we proceeded to an evaluation of the performance of the previously tested algorithms also in terms of accuracy.

An image segmentation accuracy measure is a similarity measure, defined according to the VOC challenge rules [4] as the degree of overlap between the set of segments resulted from the image segmentation algorithm and the ground truth (image segmentation masks computed by hand, provided for reference). Alternative measures include the *F-measure* [5]. The mathematical formula of the overlap measure is the following:

$$\text{Overlap}(S, G) = \frac{|S \cap G|}{|S \cup G|}$$

where  $S$  is the set of pixel masks (segments) resulted from the segmentation algorithm and  $G$  is the set of ground truth segments.

The results are presented in table 8. One aspect worth noting here is that the overlap measure is global in that it quantifies the performance of CPMC as a whole (so far, we

have presented running times for graph cuts in the figure-ground segmentation stage of CPMC).

The difference between the accuracy of CPMC running the push-relabel algorithm on supergraphs mapped on a cluster of GPU boards to that of the pseudoflow algorithm is around 1% and can be probably accounted to the fact that a pseudoflow algorithm is a bit less precise than a push-relabel algorithm. Anyhow, the main point of this experiment is to show that the NVIDIA implementation can provide reliable, high quality segments for CPMC. The comparison to the pseudoflow figures ascertains that.

	Pseudoflow	Push-relabel on GPU cluster
Avg. overlap (20 $\lambda$ )	0.733	0.744
Avg. overlap (10 $\lambda$ )	0.719	0.732

**Table 8.** Image segmentation performance of CPMC in terms of intersection over union overlap.

Another interesting point is that halving the  $\lambda$ -schedule affects the accuracy of the supergraph based solution by roughly 1%, a decrease that might be acceptable when trading off speed for accuracy. Tables 6, 7 and 8 show that by using fewer  $\lambda$ s the average times drop by roughly 28% (one seed supergraphs) and 25% (two seed supergraphs), respectively, for a loss around 1% in segmentation accuracy.

Time	Min	Avg	Max
20 $\lambda$ parfor	5.69 s	15.46 s	30.55 s
20 $\lambda$ dynamic	3.46 s	12.15 s	22.36 s
10 $\lambda$ parfor	2.96 s	11.05 s	19.26 s
10 $\lambda$ dynamic	2.61 s	9.12 s	16.18 s

**Table 9.** Static vs dynamic scheduling.

#### 4.9 Static vs. Dynamic Scheduling

As pointed out in §3.3.1, we schedule parametric max flow computations on supergraphs using a FIFO ordered, dynamically managed list of computing servers. By contrast, a static solution would assign each iteration of a *parfor* MATLAB loop computing parametric max flows to a given server in the list. We instrumented an experiment using a *parfor* loop with five threads and all of the five GPU boards on all of our four workstations, using the same setup as in §4.7. Each *parfor* iteration is statically scheduled *mod* 5 to run supergraph max flows on one of the five GPU boards. We used two seed supergraphs and  $\lambda$ -schedules of 10 and 20 values. Table 9 shows the results compared to those of the dynamic solution (the last rows of tables 6 and 7). As it can be noticed, dynamic scheduling improves average times over static solutions by almost 22% for 20  $\lambda$ -schedules and almost 18% for 10  $\lambda$ -schedules.

### 5 Conclusions

In this paper we have presented a general, parallel framework for parametric maximum flow problems in image seg-

mentation that can run on various platforms (multi-core, GPU), either locally or distributed in a cluster. In the absence of any known parallel parametric maximum flow algorithms, we proposed the concept of supergraphs to approximate parallel parametric maximum flow behavior. The framework is also useful as an evaluation tool for the available parallel maximum flow implementations [1, 2, 3]. We used such a software, namely NVIDIA’s GPU implementation of the push relabel maximum flow algorithm, together with CPMC [10], a state-of-the-art image segmentation algorithm, as a case study that points out the utility of our framework. The evaluation has shown that our solution achieves competitive max-flow computation times, without any loss of segmentation accuracy. This paves the way for a real-time solution, given that faster implementations of parallel graph cuts will become available in the near future.

## Acknowledgements

This work was supported in part by CNCS-UEFISCDI under CT-ERC-2012-1, PCE-2011-3-0438, and JRP-RO-FR-2014-16. The authors would like to thank NVIDIA Corporation for their generous hardware donation.

## References

- [1] Gridcut, fast graph-cuts for grids. <http://gridcut.com>.
- [2] Nvidia cuda library documentation. [http://graphics.im.ntu.edu.tw/~bossliaw/nvCuda\\_doxxygen/html/group\\_\\_image\\_\\_labeling\\_\\_and\\_\\_segmentation.html](http://graphics.im.ntu.edu.tw/~bossliaw/nvCuda_doxxygen/html/group__image__labeling__and__segmentation.html).
- [3] Nvidia npp library documentation. <http://docs.nvidia.com/cuda/npp/index.html#abstract>.
- [4] The pascal visual object classes homepage. <http://pascallin.ecs.soton.ac.uk/challenges/VOC/>.
- [5] S. Alpert, M. Galun, R. Basri, and A. Brandt. Image Segmentation by Probabilistic Bottom-Up Aggregation and Cue Integration. In *Proceedings of the IEEE International Conference on Computer Vision and Pattern Recognition*, 2007.
- [6] M. Babenko and A. Goldberg. Experimental Evaluation of a Parametric Flow Algorithm. Technical Report MSR-TR-2006-77, Microsoft, 2006.
- [7] Y. Boykov and V. Kolmogorov. An experimental comparison of min-cut/max-flow algorithms for energy minimization in vision. *IEEE Transactions on Pattern Analysis and Machine Intelligence*, 26(9):1124–1137, September 2004.
- [8] Y. Boykov and O. Veksler. Graph cuts in vision and graphics: Theories and applications. In N. Paragios, Y. Chen, and O. Faugeras, editors, *Handbook of Mathematical Models in Computer Vision*. Springer, 2006.
- [9] J. Carreira and C. Sminchisescu. Constrained parametric min-cuts for automatic object segmentation, release 1. <http://www.maths.lth.se/matematiklth/personal/sminchis/code/cpmc/index.html>.
- [10] J. Carreira and C. Sminchisescu. Constrained Parametric Min-Cuts for Automatic Object Segmentation. In *Proceedings of the IEEE International Conference on Computer Vision and Pattern Recognition*, June 2010.
- [11] W. Cook, W. Cunningham, W. Pulleyblank, and A. Schrijver. *Combinatorial Optimization*. John Wiley & Sons, 1998.
- [12] L. Ford and D. Fulkerson. *Flows in Networks*. Princeton University Press, 1962.
- [13] G. Gallo, M.D. Grigoriadis, and R.E. Tarjan. A fast parametric maximum-flow algorithm and applications. *SIAM Journal of Computing*, 18:3–55, February 1989.
- [14] A. Goldberg and R.E. Tarjan. A new approach to the maximum-flow problem. *Journal of the Association for Computing Machinery*, 35(4):921–940, October 1988.
- [15] D. Greig, B. Porteous, and A. Seheult. Exact maximum a posteriori estimation for binary images. *Journal of the Royal Statistical Society, Series B*, 51(2):217–279, 1989.
- [16] D. S. Hochbaum. The pseudoflow algorithm: A new algorithm for the maximum-flow problem. *Operations Research*, 56:992–1009, July 2008.
- [17] M. Hussein, A. Varshney, and L. Davis. On Implementing Graph Cuts on CUDA. In *First Workshop on General Purpose Processing on Graphics Processing Units*, Boston, MA, October 2007.
- [18] C. Ionescu, D. Papava, V. Olaru, and C. Sminchisescu. Human3.6m: Large scale datasets and predictive methods for 3d human sensing in natural environments. *IEEE Transactions on Pattern Analysis and Machine Intelligence*, 36(7):1325–1339, July 2014.
- [19] O. Jamriska, D. Sykora, and A. Hornung. Cache-efficient Graph Cuts on Structured Grids. In *Proceedings of the IEEE International Conference on Computer Vision and Pattern Recognition*, 2012.

- [20] V. Kolmogorov, Y. Boykov, and C. Rother. Applications of parametric maxflow in computer vision. In *Proceedings of the 11th IEEE International Conference on Computer Vision*, October 2007.
- [21] J. Liu and J. Sun. Parallel Graph-cuts by Adaptive Bottom-up Merging. In *Proceedings of the IEEE International Conference on Computer Vision and Pattern Recognition*, June 2010.
- [22] T. Stich. Nvidia. Personal communication.
- [23] V. Vineeth and P. J. Narayanan. CUDA Cuts: Fast Graph Cuts on the GPU. In *CVPR Workshop on Visual Computer Vision on GPUs*, Anchorage, USA, June 2008.
- [24] J. Yuan, E. Bae, X.-C. Tai, and Y. Boycov. A study on continuous max-flow and min-cut approaches. Technical Report CAM-10-61, UCLA, 2010.
- [25] J. Yuan, E. Bae, and X.C. Tai. A study on continuous max-flow and min-cut approaches. In *Proceedings of the IEEE International Conference on Computer Vision and Pattern Recognition*, June 2010.